Growth mechanisms and near-interface structure in relation to orientation of MoS_2 sputtered thin films

J. Moser and F. Lévy
Institut de Physique Appliquée, Ecole Polytechnique Fédérale, CH-1015 Lausanne, Switzerland

(Received 2 July 1991; accepted 21 October 1991)

The growth of sputter-deposited MoS_2 thin films is investigated by high-resolution transmission electron microscopy. Pure high-temperature grown films are compared with H_2O-contaminated films and amorphous annealed films. In the first case, the films are oriented. They have a first interface layer with crystallites having their (002) planes parallel with the substrate. The subsequent growth leads to the already described lamellar structure, with flakes perpendicular to the substrate. This structure can be explained in terms of a local branching process during crystal growth. The orientation relations between the crystallites in the parallel layer and the lamellae are determined. The local structure at the root of the lamellae, as well as at the interface, is investigated by image calculation. Water contamination in the plasma is shown to result in an amorphization of the interfacial region, followed by lamellar growth. Amorphous films annealed under vacuum do not show a lamellar structure, but have isotropic crystallization. In each of these cases, the mechanism determining the film structure is different.

I. INTRODUCTION

The orientation of basal planes in lubricating MoS_2 thin films is the subject of many recent studies. Usually, sputtered MoS_2 thin films are known to have a lamellar hexagonal structure, with basal (002) planes perpendicular to the substrate.[1–3] With different methods, some authors succeeded in producing films with basal planes parallel with the substrate.[4–9] The advantages of such films are a better stability with respect to oxidation and an orientation of the basal planes directly in the sliding direction of the substrate, resulting in an increased wear life.[9] Basal plane orientation is also important in thin films of other similar layered materials for various applications. A recent example is TiS_2 thin films, whose charge accumulation properties in Li batteries depend on crystalline orientation.[10] Many authors use chemical characterization to investigate the mechanisms determining this orientation. The most promising explanation, proposed by Buck, relates to the water partial pressure during deposition.[5–7] Recently, a more complex situation has been described: the morphology results from the succession of both orientations during the growth of the film.[11] The aim of this paper is to provide a precise structural description of the interfacial region. A powerful means for this purpose is high-resolution transmission electron microscopy (HRTEM), with the beam parallel (cross section) or perpendicular (top view) to the interface. Structure models can be tested using computer image simulation and comparing results with experimental images.

II. EXPERIMENTAL

MoS_2 thin films are deposited by RF-magnetron sputtering. Substrates are Si[100], for cross-sectional TEM observation, and amorphous C films on Au grids for top-view TEM observation. Si substrates are covered by a thin amorphous layer of native SiO_2. The deposition parameters are substrate temperature from room temperature to 500 °C, Ar pressure 2.2 Pa, RF power density 10 W cm^{-2}, and distance between target and substrate 9.5 cm. The target is a commercial one, hot-pressed from powder, 99% pure, effective diameter 38 mm. The pumping system includes a cryogenic trap to reduce the partial pressure of H_2O vapor. The pressure can be lowered before deposition down to 10^{-7} Pa, in static conditions and at ambient temperature. In order to study the effect of H_2O partial pressure on the film structure, H_2O vapor can be introduced into the chamber as a reactive gas with a pressure ranging from 10^{-4} to 10^{-1} Pa.

Cross sections for TEM observation are prepared by mechanical polishing, followed by ion-milling. The sample is etched until a hole forms at its center. The film is observed at the edge of the hole. The observation is performed using a Philips EM 430 TEM at 300 kV. Computed HRTEM images are generated using the program EMS.[12] The calculation principle is the multislice method.[13] The slice thickness Δz is typically less than 0.5 nm. The wave at the exit face of the sample is modulated

 © 1992 Materials Research Society
Downloaded from https://www.cambridge.org/core. University of Basel Library, on 30 May 2017 at 20:08:01, subject to the Cambridge Core terms of use, available at https://www.cambridge.org/core/terms. https://doi.org/10.1557/JMR.1992.0734

by the contrast transfer function (CTF) of the microscope. The image characteristics are sensitive to sample thickness, defocus, and other parameters which are, for the EM 430 ST at 300 kV, defocus spread 16 nm, beam convergency 1.6 mrad, and spherical aberration coefficient $C_s = 2$ mm.

III. RESULTS AND DISCUSSION

A. General structure

Figure 1 shows a low-magnification cross-sectional view of a MoS_2 thin film deposited on Si[100], together with the corresponding diffraction pattern. The deposition temperature was 300 °C. The upper part of the film is made of lamellae perpendicular to the substrate. The density, determined by film weight and thickness measurement, is low ($\rho \simeq \rho_{\mathrm{bulk}}/3$), because of the presence of voids between lamellae. Close to the interface, a thin zone, more compact, is visible. The thin white line between MoS_2 and Si is native amorphous silicon oxide.

Higher magnification reveals the connection between morphology and crystalline structure (Fig. 2). Fringes corresponding to (002) planes, with ~6 Å spacing, are visible on the picture. Near the interface, the dense zone is made of crystallites oriented with their (002) planes parallel with the substrate, whereas in the upper part of the film the lamellae contain crystallites having their (002) planes mostly perpendicular to the substrate. The thickness of the dense parallel zone is equal to 5–10 times the (002) lattice plane spacing (3–6 nm). This general structure is present independently from the degree of crystallization, which itself increases with the deposition temperature.

B. First stages of growth

Figure 3 shows a very thin MoS_2 film on Si, with (002) lattice planes visible. Its thickness is 1–2 nm, constant over wide areas. It indicates a very fast surface covering, which can be explained by the high growth velocity in the [*uv*0] directions.

Figure 4 is a high magnification view of the interfacial region of a sample similar to those of Figs. 1 and 2. Its main features are, first, the parallel layer with the interface and, second, the root of a lamella growing from the parallel layer. The interface between silicon oxide and MoS_2 is well defined. Two simple interface models can be tested using HRTEM image calculations. In the first model, a MoS_2 crystal lies on the silicon oxide surface. The S surface being weakly reactive, the average separation between oxide surface and MoS_2 has been taken approximately equal to the distance separating two adjacent S planes in a MoS_2 crystal. In the second one, the first S plane of the MoS_2 crystal has been removed, leading to a more reactive interface between silicon oxide and a Mo plane. The distance between both phases is smaller (approximately 1 Å). The amorphous silicon oxide layer itself has been modeled as a random distribution of Si and O atoms in cells, each one containing three SiO_2 molecules. The cell volume was defined in

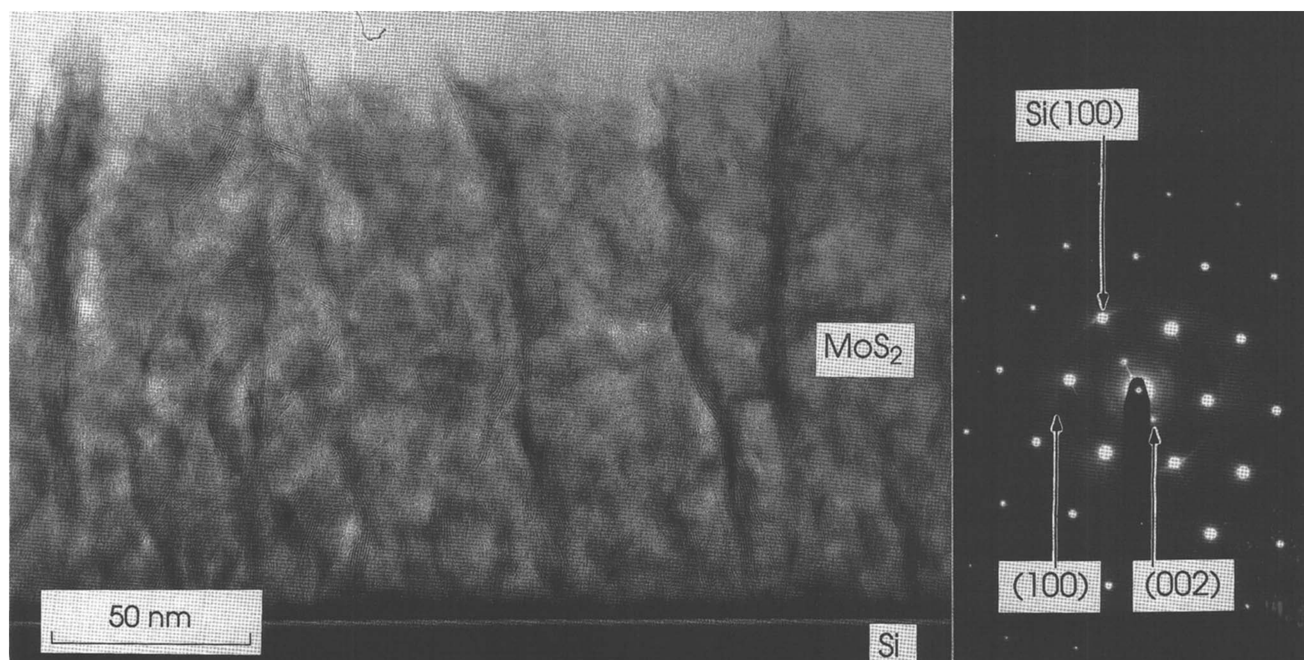

FIG. 1. Low magnification TEM micrograph and electron diffraction pattern of a MoS_2 thin film on Si[100]. The electron beam is parallel with the interface (cross section).

Downloaded from https://www.cambridge.org/core. University of Basel Library, on 30 May 2017 at 20:08:01, subject to the Cambridge Core terms of use, available at https://www.cambridge.org/core/terms. https://doi.org/10.1557/JMR.1992.0734

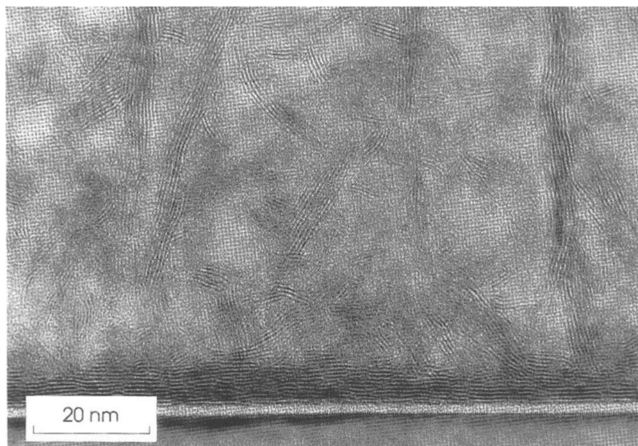

FIG. 2. TEM cross-sectional micrograph of a MoS_2 film on Si[100]. The fringes correspond to MoS_2 (002) planes. The amorphous zone between Si and MoS_2 is silicon oxide.

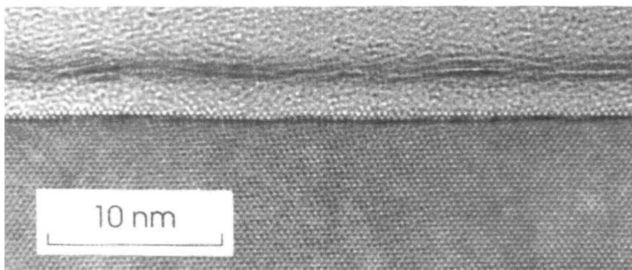

FIG. 3. TEM cross-sectional micrograph of a very thin MoS_2 film (1–2 nm thick). The film is completely continuous.

order to reproduce the density of the material. The results are shown in Fig. 5. The zone axis for MoS_2 is [100], although the general direction of observation in real cases is [$uv0$]. For thin samples and near the Scherzer defocus, the main features of the calculated image do not show a strong dependence on thickness and defocus. For the MoS_2 crystal, bright (002) fringes with ~6 Å periodicity fill the empty spaces between adjacent S planes. The image details in the direction parallel with these fringes may be different in real images because of the random orientation of crystallites around their $\vec{c}$ axis. In the first model, a last bright fringe fills the empty space between MoS_2 and the amorphous oxide. Its distance from the previous one is also close to 6 Å. In the second one, the fringe between the two materials is less defined, and its distance from the previous one is shorter. The first model can be recognized at many places along the interface on Fig. 4. At other sites, the aspect of the interface does not allow for a distinction between the second model and an effect of substrate roughness along the direction of observation.

C. Growth of lamellae

The crystalline orientation relationships between the lamellae in their first stages of growth and the underlying crystallites in the parallel layer can be determined using electron diffraction and HRTEM. When the film is thin enough, i.e., if the lamellae are small enough, the (002) lattice planes of the lamellae tend to be parallel with the (100) planes of the underlying parallel crystals. This is illustrated in Fig. 6, which is a high magnification detail

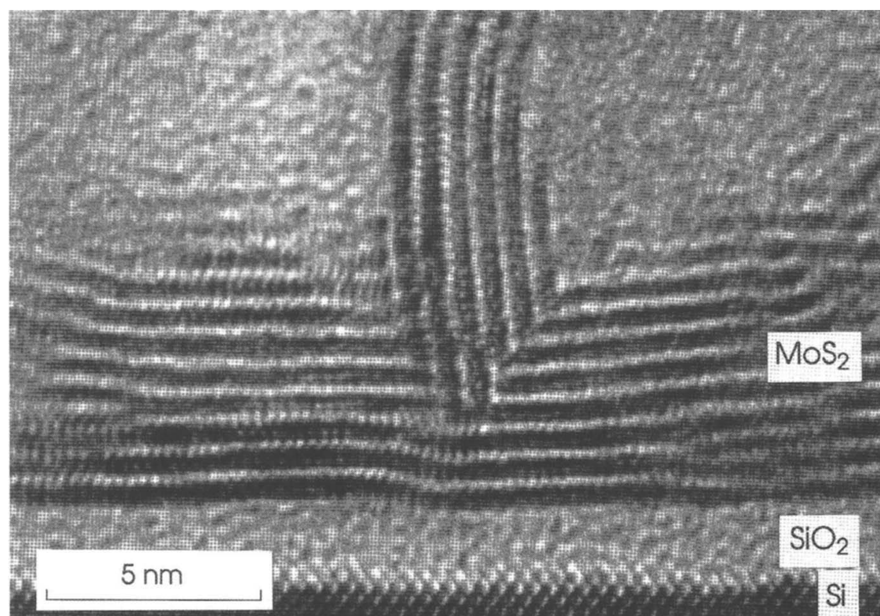

FIG. 4. High-resolution TEM micrograph of the interfacial region of the film of Figs. 1 and 2 (cross section). The image shows, first, the interface between silicon oxide and the first MoS_2 layer, and second, the root of a lamella. White fringes correspond to MoS_2 (002) planes.

Downloaded from https://www.cambridge.org/core. University of Basel Library, on 30 May 2017 at 20:08:01, subject to the Cambridge Core terms of use, available at https://www.cambridge.org/core/terms. https://doi.org/10.1557/JMR.1992.0734

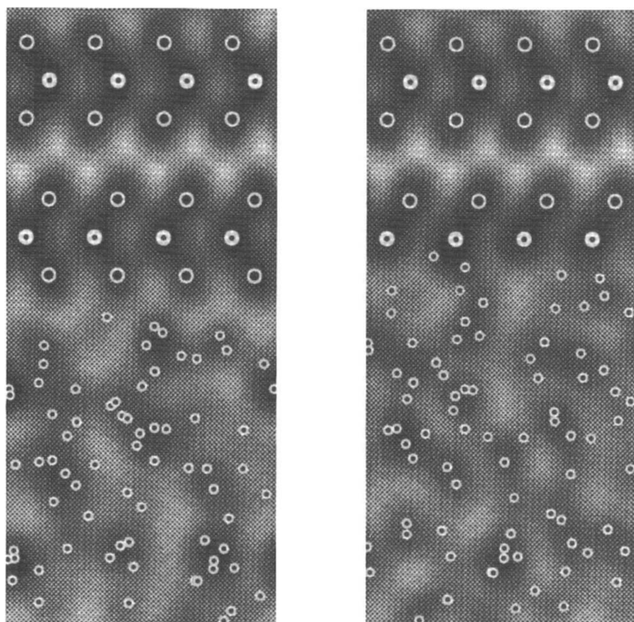

FIG. 5. Computed HRTEM images corresponding to different interface models. Bottom: amorphous SiO_2; top: MoS_2 crystal. The circles indicate atom positions.

of a MoS_2 film deposited on amorphous carbon, seen along an axis perpendicular to the interface. This result is confirmed by a statistical study on several lamellae. The electron diffraction pattern of Fig. 1 shows diffraction spots due to the Si substrate and rings corresponding to the MoS_2 film. The zone axis for Si is [110]. The MoS_2 (002) ring is separated in two parts, corresponding to the two main crystallite orientations—parallel or perpendicular to the substrate. The (100) ring is primarily due to lamellae having their $\vec{c}$ axis parallel with the electron beam. Its inhomogeneity indicates that the corresponding crystallites tend to have their (100) planes parallel with the interface. These orientation relationships are summarized in Table I. Figure 7 is a schematic model of the local situation. The exact position of the lamella is arbitrary. The two crystals show a lattice coincidence, with a periodicity a_0, along a common [100]. This suggests the presence of a chemical bonding along a contact line parallel with this direction. Observation of well-crystallized films shows the occurrence of this branching mechanism also in the bulk of the film, leading to complex dendritic-like structures (Fig. 8).

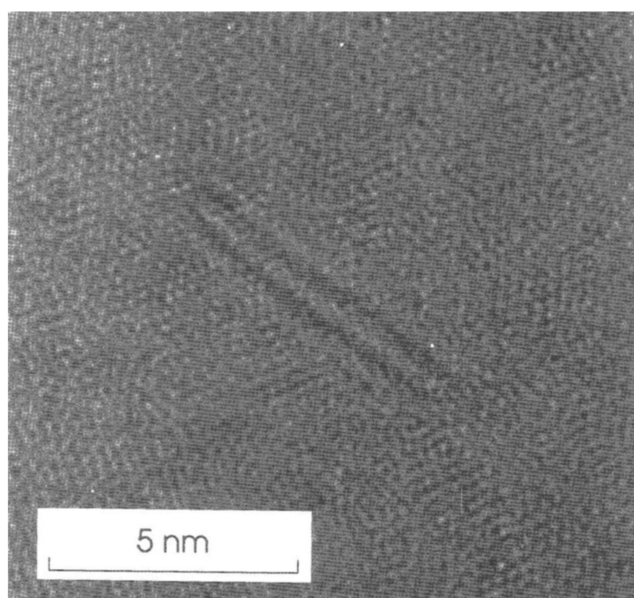

FIG. 6. High-resolution TEM micrograph of a very thin MoS_2 film showing the early growth of a lamella. The electron beam is perpendicular to the interface (top view).

Information about the structure at the basis of the lamellae can be extracted from the fringe pattern of Fig. 4. At the root of the lamella, the horizontal white fringe is interrupted. Image calculations show that it can be due to a filling of the empty space between S planes. Two simplified models are shown on Fig. 9 with the corresponding calculated fringe pattern. They do not pretend to give an exact atom position or to be chemically realistic. Neither do they take into account the presence of impurities. The S surfaces being weakly reactive, the first model considers a lamella bonded to the parallel layer through interaction with a Mo plane. It was arbitrarily decided to replace an array of S atoms in a [100] direction by the Mo atoms of the lamella. In the second model, there is an empty space above the S surface. The lamella is not strongly bonded to the underlying crystal. The fringe pattern of model one is similar, in its main features, to the experimental image. Furthermore, this model, with a lamella bonded along a line, is consistent with the matching of the interatomic spacings in both crystals along the bonding line.

D. Influence of partial H_2O pressure

Films have been deposited in the presence of variable amounts of H_2O vapor in the chamber atmosphere.

TABLE I. Relative crystalline orientations in the branching process.

A		B
(002)	⊥	(002)
(002)	||	(100)
(100)	||	(002)

A: Old crystal.
B: New crystal.

Downloaded from https://www.cambridge.org/core. University of Basel Library, on 30 May 2017 at 20:08:01, subject to the Cambridge Core terms of use, available at https://www.cambridge.org/core/terms. https://doi.org/10.1557/JMR.1992.0734

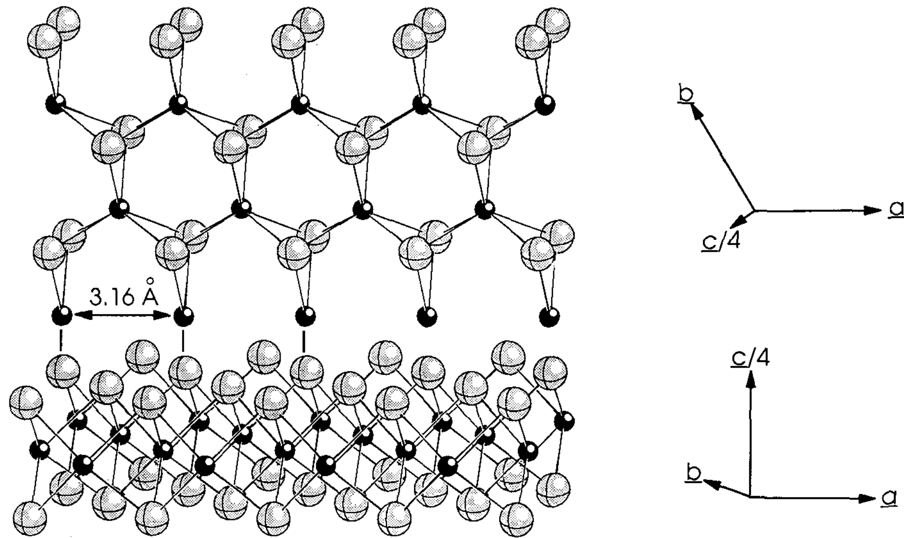

FIG. 7. Schematic model of the crystalline orientations in the branching process. The exact relative positions of both crystals are arbitrary.

For H_2O pressures up to $5 \cdot 10^{-3}$ Pa, the film structure does not show any changes; the interface remains well crystallized. With $1.3 \cdot 10^{-2}$ Pa H_2O, a partial amorphization of the interfacial region occurs (Fig. 10). With $5 \cdot 10^{-2}$ Pa H_2O, a dense, amorphous region extends from the interface over 40 nm. Subsequent crystallization occurs gradually, leading to randomly oriented crystallites. Those oriented with [*uv*0] directions perpendicular to the substrate can grow without obstacles and lead to the lamellar structure in the outer part of the film. At H_2O pressures higher than 10^{-1} Pa, the films are completely amorphous.

FIG. 8. Cross-sectional TEM micrograph of MoS_2 crystals in the bulk of the film, showing the dendritic-like structure induced by the branching processes.

E. Annealed films

The structure of MoS_2 thin films is strongly related to the growth mechanisms. High-temperature grown films can be compared with films deposited at low temperature and low power and annealed under vacuum at 500 °C for 1 h. Before annealing, these

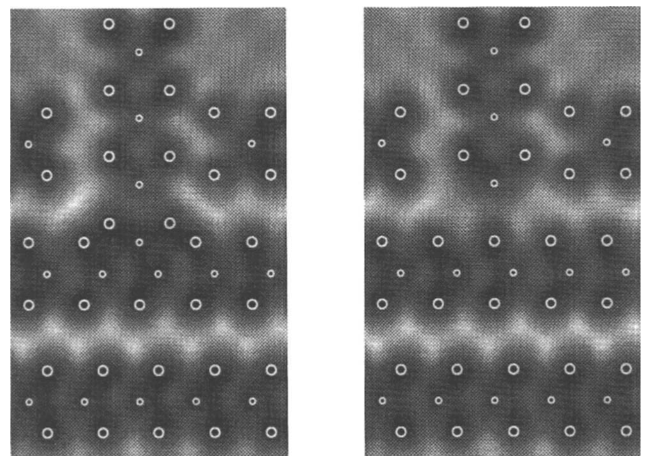

FIG. 9. Computed HRTEM images of the root of a lamella, from two different models (see Fig. 4). The circles indicate atom positions.

Downloaded from https:/www.cambridge.org/core. University of Basel Library, on 30 May 2017 at 20:08:01, subject to the Cambridge Core terms of use, available at https:/www.cambridge.org/core/terms. https://doi.org/10.1557/JMR.1992.0734

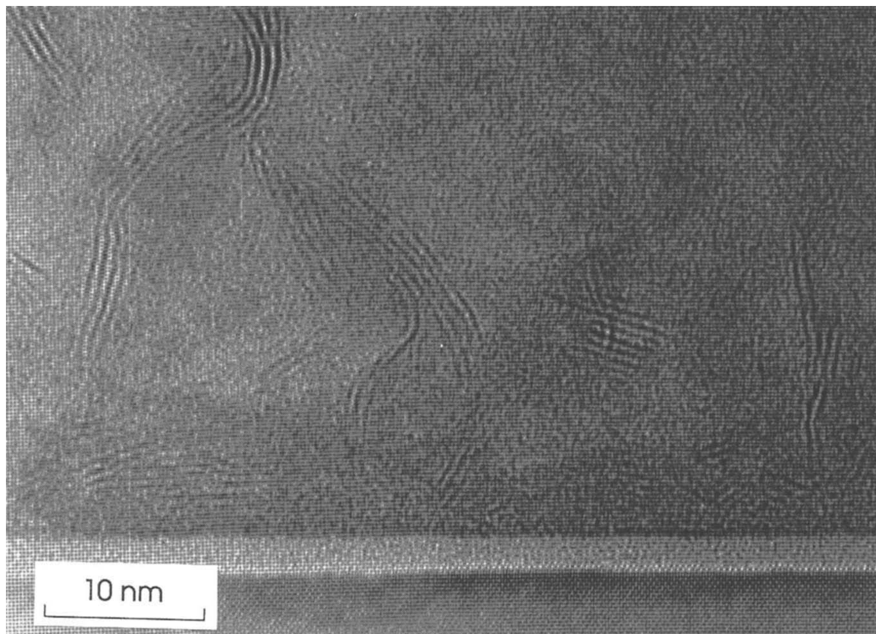

(a)

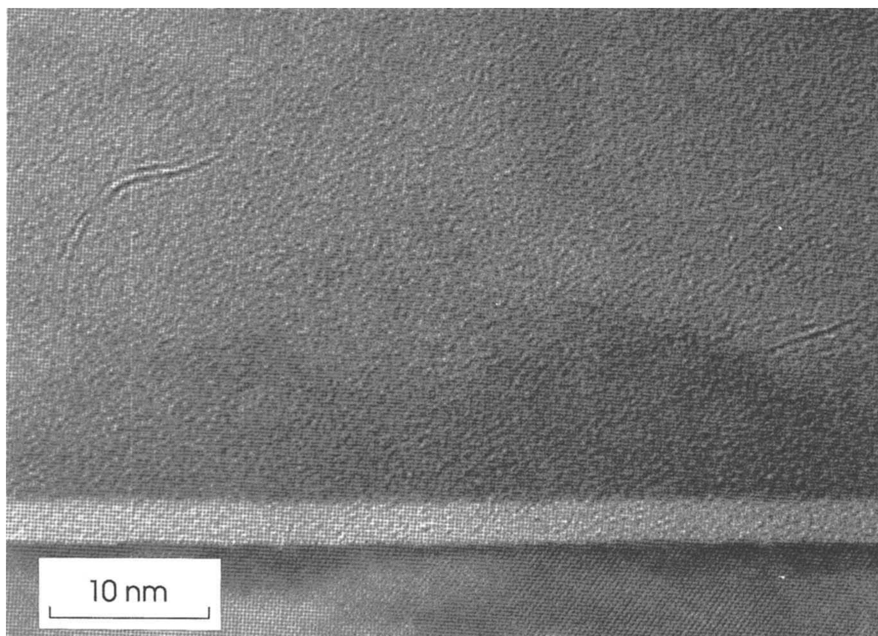

(b)

FIG. 10. Cross-sectional TEM micrograph of the interface of MoS_2thin films contaminated during deposition by different amounts of water vapor: (a) $1.3 \cdot 10^{-2}$ Pa and (b) $5.3 \cdot 10^{-2}$ Pa.

films were shown to be amorphous by x-ray diffraction measurements. The structure after annealing is shown in Fig. 11. No lamellar structure is apparent. Crystallites are randomly oriented in the whole film, even at the interface. The interface is rougher than in films deposited at 500 °C, where the presence of the inert S layer inhibits the thermally activated diffusion or chemical reaction at the interface. In the case of an amorphous film such phenomena are allowed by the presence of dangling bonds near the interface.

IV. CONCLUSION

The structure of sputtered MoS_2 thin films is strongly related to the growth and crystallization mechanisms. For films deposited under pure argon and high substrate

Downloaded from https:/www.cambridge.org/core. University of Basel Library, on 30 May 2017 at 20:08:01, subject to the Cambridge Core terms of use, available at https:/www.cambridge.org/core/terms. https://doi.org/10.1557/JMR.1992.0734

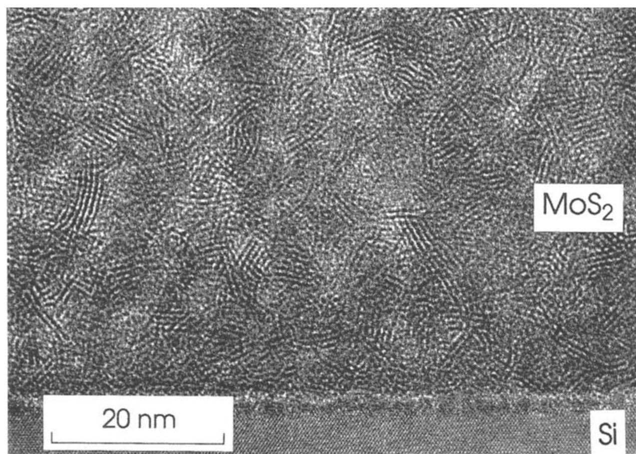

FIG. 11. Cross-sectional TEM micrograph of an originally amorphous MoS_2 thin film after 1 h annealing under vacuum at 500 °C.

temperature, the films are crystallized. The crystallites at the interface have their (002) planes parallel with the substrate. They form a uniform coverage, a few nanometers thick. Crystal growth is characterized by branching processes with epitaxial characteristics. Occurring during the growth of the parallel layer near the interface, this process leads to the growth of crystallites having their (002) planes perpendicular to the substrate. If the degree of crystallization is high enough, i.e., if the length of crystallites is of the same order of magnitude as the film thickness, the lamellar morphology appears, characterized by the presence of vertical flakes. Branching can be observed also from crystallites in the bulk of the film, as described by Buck[7] under the term "dendritic growth". This kind of structure has been observed for all substrate temperatures, provided that they were high enough for the film to be crystallized. Water contamination during deposition leads to films with an amorphous interface. Crystallization occurs during the subsequent stages of growth in an isotropic way. The final lamellar morphology of these films is the result of a geometrical selection mechanism. The crystals having their growth directions [*uv*0] perpendicular to the substrate grow without obstacles, whereas the growth of differently oriented crystals is limited. The annealing of amorphous films leads to an isotropic crystallization in the whole thickness without lamellar morphology, and to a diffused interface.

To conclude, we can point out that, besides the geometrical description of the growth phenomena present in this paper, an alternative approach might consist of an explanation based on energetic or thermodynamic arguments.

ACKNOWLEDGMENTS

This work has been financially supported by the Fondation Suisse pour la Recherche en Microtechnique and by the Fonds National Suisse de la Recherche Scientifique.

REFERENCES

1. R. Bichsel, P. Buffat, and F. Lévy, J. Phys. D: Appl. Phys. **19**, 1575–1585 (1986).
2. J.R. Lince and P.D. Fleischauer, J. Mater. Res. **2**, 827–838 (1987).
3. V. Buck, Wear **91**, 281–288 (1983).
4. A. Aubert, J.P. Nabot, J. Ernoult, and Ph. Renaux, *Proc. 7th Int. Conf. on Ion and Plasma Assisted Techniques,* 281–286 (1989).
5. V. Buck, Thin Solid Films **139**, 157–168 (1986).
6. V. Buck, Vacuum **36**, 89–94 (1986).
7. V. Buck, Wear **114**, 263–274 (1987).
8. P.A. Bertrand, J. Mater. Res. **4**, 180–184 (1989).
9. P.D. Fleischauer, ASLE Trans. **27** (1), 82–88 (1983).
10. S. Kikkawa, M. Miyazaki, and M. Koizumi, J. Mater. Res. **5**, 2894–2901 (1990).
11. J. Moser, H. Liao, and F. Lévy, J. Phys. D: Appl. Phys. **23**, 624–626 (1990).
12. P.A. Stadelmann, Ultramicroscopy **21**, 131–146 (1987).
13. P. Goodman and A.F. Moodie, Acta Cryst. **A30**, 280–290 (1974).

Downloaded from https://www.cambridge.org/core. University of Basel Library, on 30 May 2017 at 20:08:01, subject to the Cambridge Core terms of use, available at https://www.cambridge.org/core/terms. https://doi.org/10.1557/JMR.1992.0734